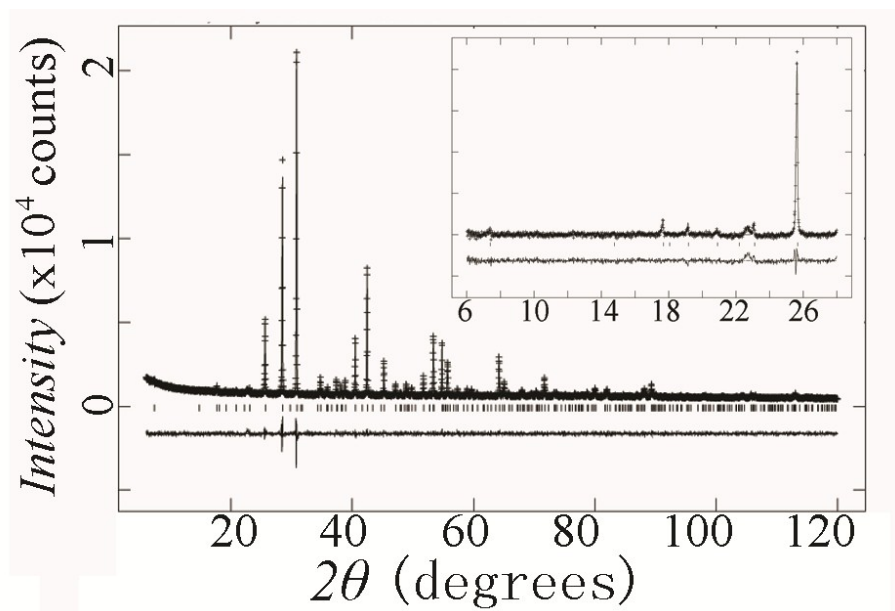


## New 10H perovskites $\text{Ba}_5\text{Ln}_{1-x}\text{Mn}_{4+y}\text{O}_{15-\delta}$ with spin glass behaviour

Congling Yin <sup>a\*</sup>, Genfang Tian <sup>b</sup>, Guobao Li <sup>c</sup>, Fuhui Liao <sup>c</sup> and Jianhua Lin <sup>c</sup>

### Supporting Information



**Figure S1.** The fitted XRD plot of the  $\text{Ba}_5\text{Sm}_{0.98}\text{Mn}_{4.01}\text{O}_{15-\delta}$  sample. The inset expands the low-angle regions

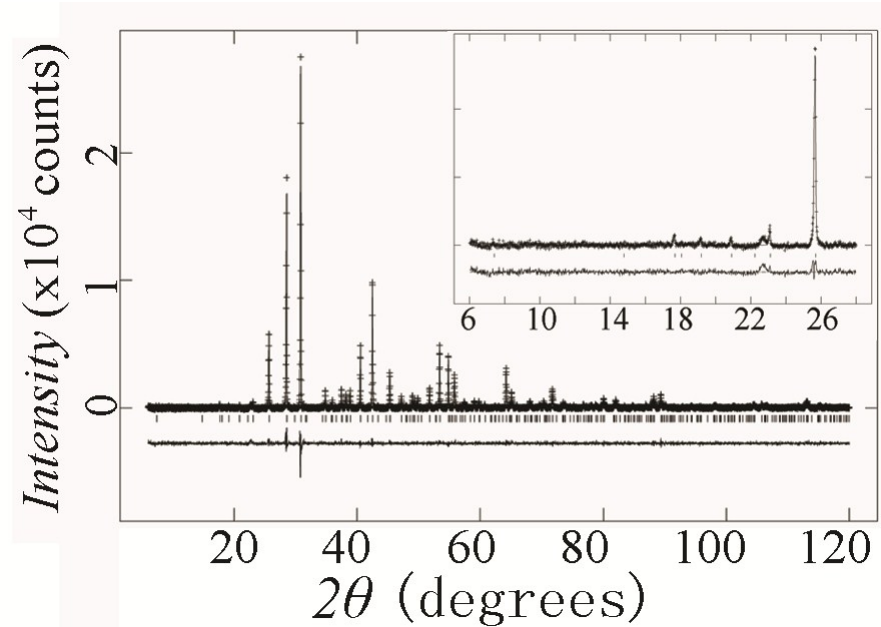


**Figure S2.** The fitted XRD plot of the  $\text{Ba}_5\text{Eu}_{0.87}\text{Mn}_{4.02}\text{O}_{15-\delta}$  sample. The inset expands the low-angle regions

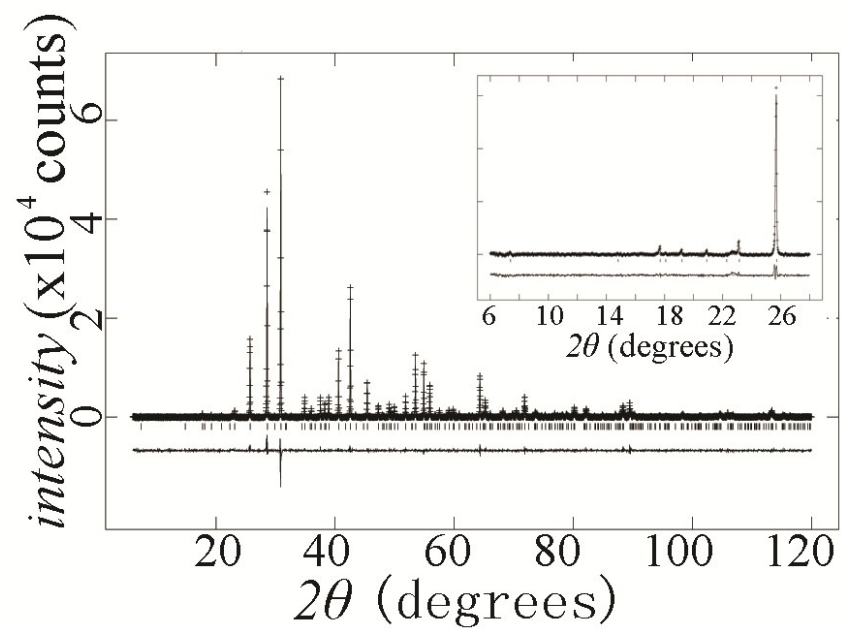


**Figure S3.** The fitted XRD plot of the  $\text{Ba}_5\text{Gd}_{0.82}\text{Mn}_{4.17}\text{O}_{15-\delta}$  sample. The inset expands the low-angle regions

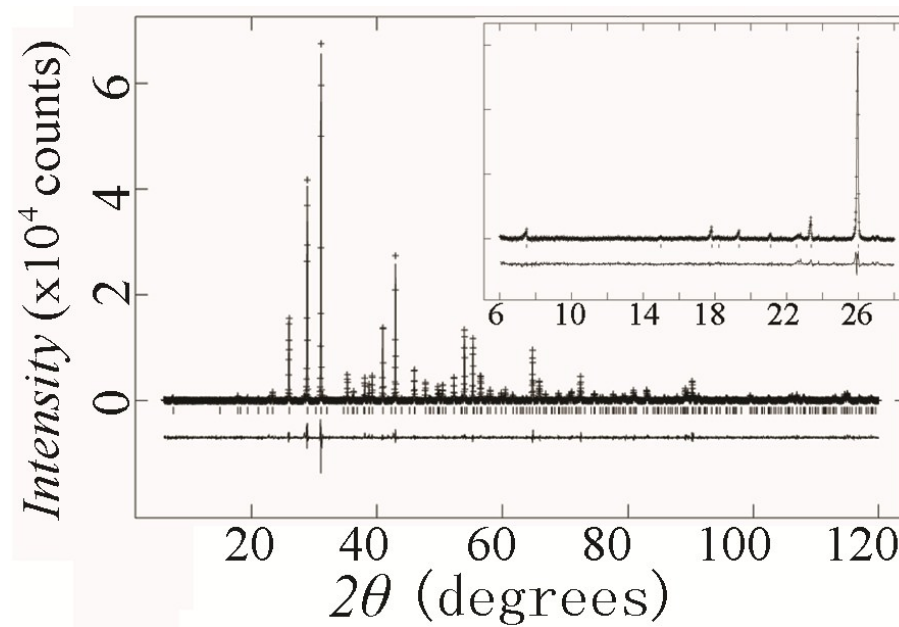


**Figure S4.** The fitted XRD plot of the  $\text{Ba}_5\text{Tb}_{0.85}\text{Mn}_{4.15}\text{O}_{15-\delta}$  sample. The inset expands the low-angle regions

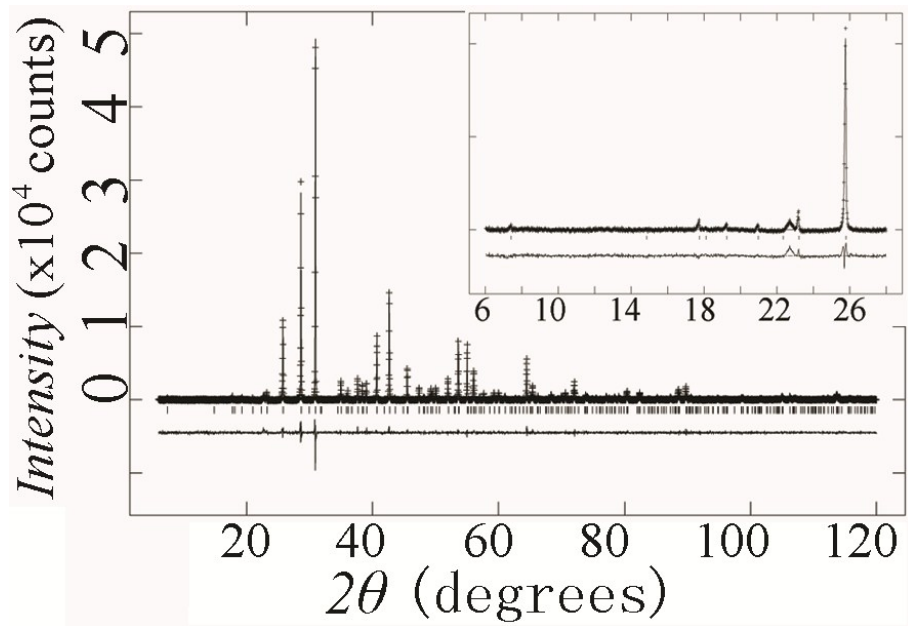


**Figure S5.** The fitted XRD plot of the  $\text{Ba}_5\text{Dy}_{0.86}\text{Mn}_{4.12}\text{O}_{15.8}$  sample. The inset expands the low-angle regions

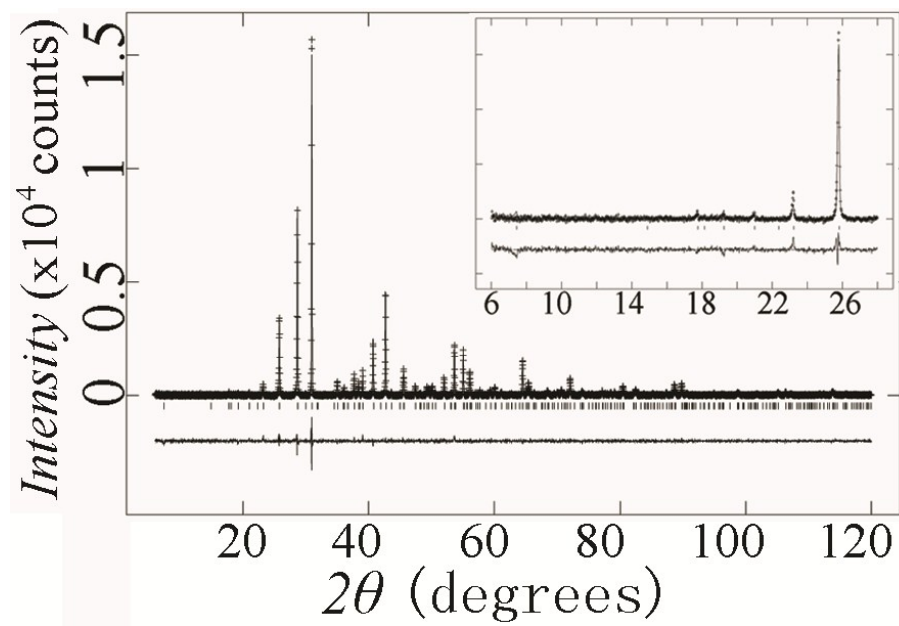


**Figure S6.** The fitted XRD plot of the  $\text{Ba}_5\text{Ho}_{0.86}\text{Mn}_{4.12}\text{O}_{15.8}$  sample. The inset expands the low-angle regions

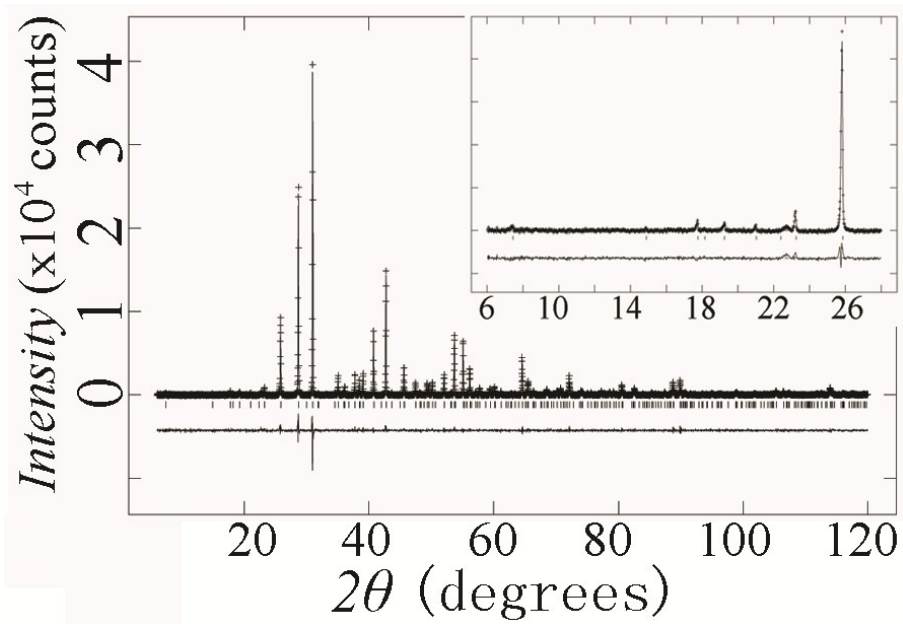


**Figure S7.** The fitted XRD plot of the  $\text{Ba}_5\text{Er}_{0.82}\text{Mn}_{4.17}\text{O}_{15-\delta}$  sample. The inset expands the low-angle regions

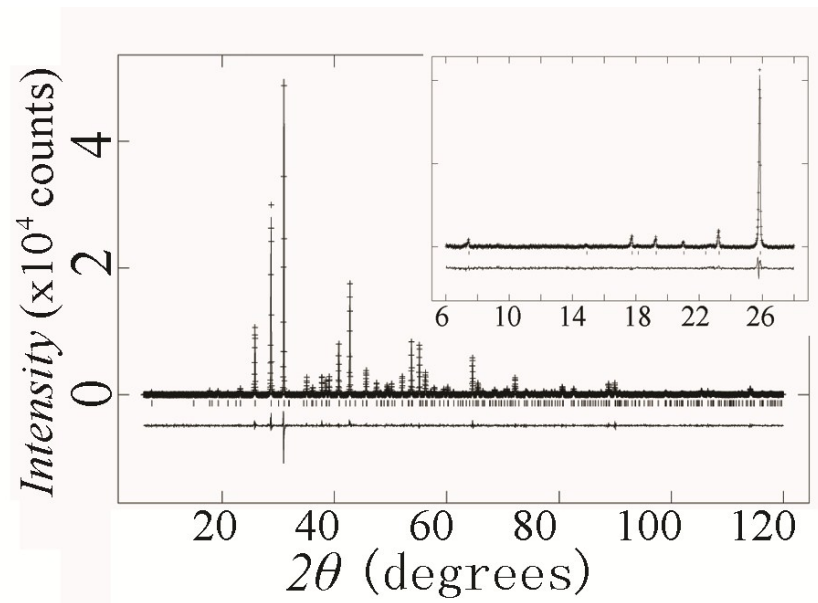


**Figure S8.** The fitted XRD plot of the  $\text{Ba}_5\text{Tm}_{0.80}\text{Mn}_{4.14}\text{O}_{15-\delta}$  sample. The inset expands the low-angle regions

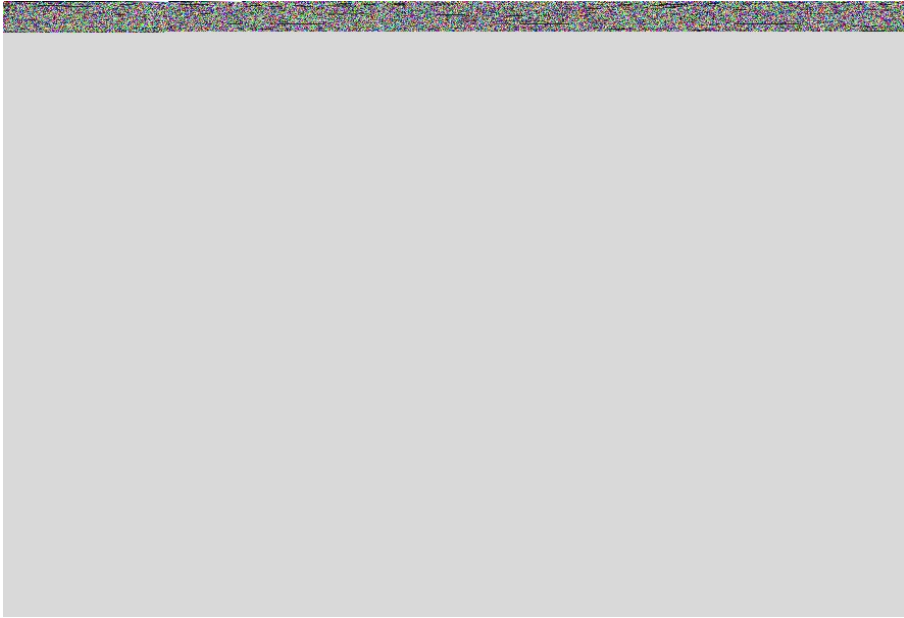


**Figure S9.** The fitted XRD plot of the  $\text{Ba}_5\text{Yb}_{0.83}\text{Mn}_{4.17}\text{O}_{15.8}$  sample. The inset expands the low-angle regions

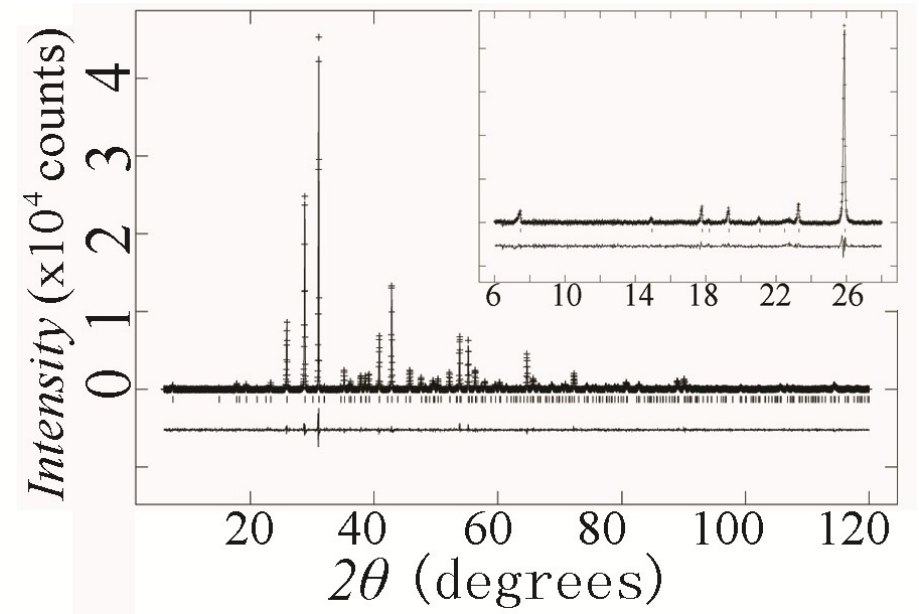


**Figure S10.** The fitted XRD plot of the  $\text{Ba}_5\text{Lu}_{0.78}\text{Mn}_{4.21}\text{O}_{15.8}$  sample. The inset expands the low-angle regions

**TABLE S1.** The structural parameters for  $Ba_5Ln_{1-x}Mn_{4+y}O_{15-\delta}$  from fits to x-ray diffraction profiles, showing lattice parameters, atomic coordinates, isotropic temperature ( $U$ ) factors for the cation sites (oxygen atom values were fixed to be 0.025 Å), and M-O and Mn-Mn distances. The structure has space group  $P6_3/mmc$ . Sites: Ba1: 2d ( $\frac{2}{3} \frac{1}{3} \frac{1}{4}$ ); Ba2: 4f ( $\frac{2}{3} \frac{1}{3} z_1$ ); Ba3: 4e (0 0  $z_2$ ); Ln: 2a(0 0  $\frac{1}{2}$ ); Mn1: 4f ( $\frac{1}{3} \frac{2}{3} z_3$ ); Mn2: 4f ( $\frac{1}{3} \frac{2}{3} z_4$ ); O1: 6h( $x_1 -x_1 \frac{1}{4}$ ); O2: 12k ( $x_2 -x_2 z_5$ ); O3: 12k ( $x_3 -x_3 z_6$ )

<i>Ln</i>	<i>a</i> /Å	<i>c</i> /Å	<i>V</i> /Å <sup>3</sup>	<i>Ba</i> 1:	<i>Ba</i> 2:	<i>Ba</i> 2:	<i>Ba</i> 3: <i>z</i> <sub>2</sub>	<i>Ba</i> 3:	<i>Ln</i> :	<i>Mn</i> 1:	<i>Mn</i> 1:	<i>Mn</i> 2:	<i>Mn</i> 2:	<i>O</i> 1: <i>x</i> <sub>1</sub>	<i>O</i> 2: <i>x</i> <sub>2</sub>	<i>O</i> 2: <i>z</i> <sub>5</sub>	<i>O</i> 3: <i>x</i> <sub>3</sub>	<i>O</i> 3: <i>z</i> <sub>6</sub>	<i>d</i> <sub>Ln-O</sub>	<i>d</i> <sup>[a]</sup> <sub>Mn1-O</sub>	<i>d</i> <sup>[a]</sup> <sub>Mn2-O</sub>	<i>d</i> <sub>Mn1-Mn2</sub>	<i>d</i> <sub>Mn2-Mn2</sub>
				100 <i>xU</i>	<i>z</i> <sub>1</sub>	100 <i>xU</i> ,/Å		100 <i>xU</i>	100 <i>xU</i>	<i>z</i> <sub>3</sub>	100 <i>xU</i> ,	<i>z</i> <sub>4</sub>	100 <i>xU</i>						/ Å	/ Å	/ Å	/ Å	/ Å
				/Å <sup>2</sup>		<sup>2</sup>		/Å <sup>2</sup>	/Å <sup>2</sup>		/Å <sup>2</sup>		/Å <sup>2</sup>										
Sm	5.7978(1)	24.0387(4)	699.79(2)	1.0(2)	0.4392(1)	1.1(1)	0.3419(1)	0.8(1)	2.1(2)	0.4040(3)	0.3(3)	0.2995(3)	2.4(3)	0.179(2)	0.177(1)	0.4445(7)	0.488(1)	0.3505(6)	2.22(1)	1.93(1)	1.97(1)	2.52(1)	2.37(1)
Eu	5.7957(1)	23.9851(3)	697.72(2)	1.5(2)	0.4396(1)	1.7(1)	0.3422(1)	1.4(1)	2.2 (2)	0.4042(3)	1.4(3)	0.2996(3)	2.8(3)	0.186(2)	0.176(2)	0.4456(7)	0.485(1)	0.3510(5)	2.20(1)	1.93(1)	1.93(1)	2.51(1)	2.38(1)
Gd	5.7898(1)	23.9556(3)	695.44(1)	1.3(1)	0.4400(1)	1.7(1)	0.3423(1)	1.5(1)	1.7(1)	0.4042(2)	1.9(2)	0.300 (3)	2.7(2)	0.183(2)	0.175(1)	0.4471(6)	0.484(1)	0.3511(5)	2.17(1)	1.93(1)	1.93(1)	2.49(1)	2.41(1)
Tb	5.7508(1)	23.6530(3)	677.44(1)	1.7(1)	0.4417(1)	1.6(1)	0.3441(1)	1.3(1)	2.6(1)	0.4060(3)	1.7(2)	0.3013(3)	2.2(2)	0.181(2)	0.172(1)	0.4490(6)	0.484(1)	0.3524(5)	2.10(1)	1.93(1)	1.94(1)	2.48(1)	2.43(1)
Dy	5.7772(2)	23.8843(6)	690.36(5)	1.3 (1)	0.4408(1)	1.6(1)	0.3427(1)	1.5(1)	2.8(1)	0.4044(3)	1.5 (3)	0.3003(3)	2.7(2)	0.181(2)	0.177(1)	0.4466(6)	0.485(1)	0.3512(5)	2.18(1)	1.92(1)	1.94(1)	2.49(1)	2.40(1)
Ho	5.7736(1)	23.8554(4)	688.66(2)	1.7(2)	0.4417(1)	1.7(1)	0.3431(1)	1.4 (1)	4.0(2)	0.4041(3)	0.4(2)	0.2993(3)	2.6(3)	0.187(2)	0.175(2)	0.4442(7)	0.480(1)	0.3502(6)	2.20(1)	1.90(1)	1.89(1)	2.50(1)	2.35(1)
Er	5.7695(1)	23.8303(3)	686.96(2)	1.4 (1)	0.4415(1)	1.6(1)	0.3432(1)	1.6(1)	2.7 (1)	0.4048(3)	1.7 (2)	0.3002(3)	2.5(2)	0.184(2)	0.175(1)	0.4473(6)	0.484(1)	0.3515(5)	2.15(1)	1.92(1)	1.93(1)	2.49(1)	2.39(1)
T	5.7658(1)	23.8029(3)	685.31(1)	1.5(1)	0.4417(1)	1.7(1)	0.3434(1)	1.6(1)	2.0(1)	0.4057(2)	2.2(2)	0.3005(3)	2.4(2)	0.184(2)	0.173(1)	0.4480(5)	0.485(1)	0.3511(5)	2.13(1)	1.94(1)	1.92(1)	2.50(1)	2.40(1)
m																							
Yb	5.7639(2)	23.766 (1)	683.80(7)	1.0 (2)	0.4424(1)	1.3 (1)	0.3440(1)	0.9(1)	1.7(2)	0.4054(3)	0.7(3)	0.2996(4)	2.5(3)	0.183(2)	0.174(2)	0.4474(9)	0.488(2)	0.3508(7)	2.14(1)	1.95(1)	1.94(1)	2.52(1)	2.36(1)
Lu	5.7573(1)	23.7459(3)	681.63(2)	2.7 (1)	0.4423(1)	2.8(1)	0.3440(1)	2.5(1)	2.6(1)	0.4062(2)	2.9(2)	0.3010(2)	3.3(2)	0.188(1)	0.172(1)	0.4490(4)	0.485(1)	0.3508(4)	2.10(1)	1.95(1)	1.90(1)	2.50(1)	2.42(1)

[a] the average bond length

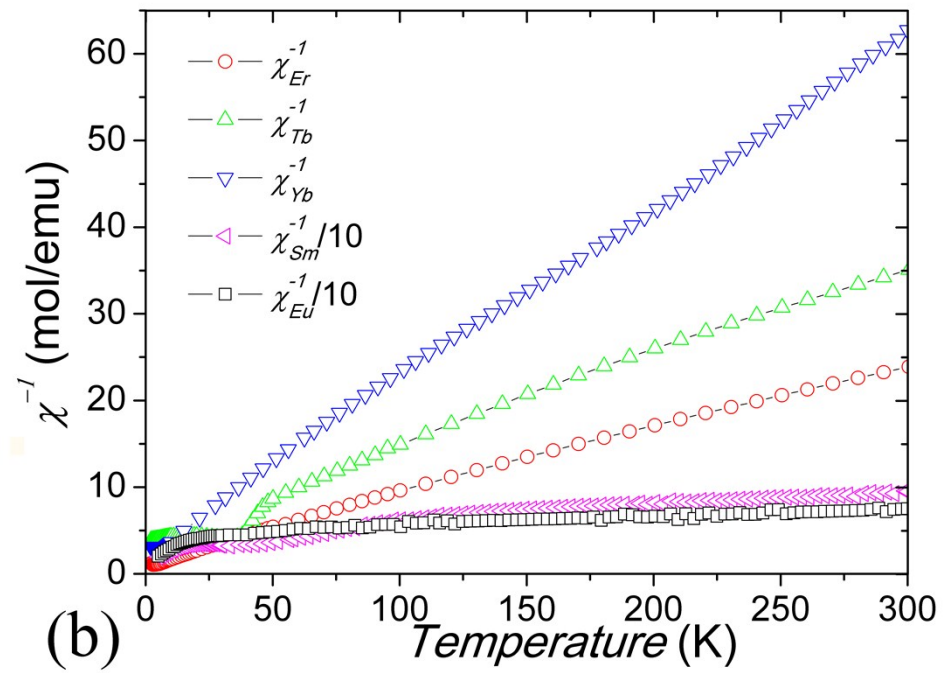
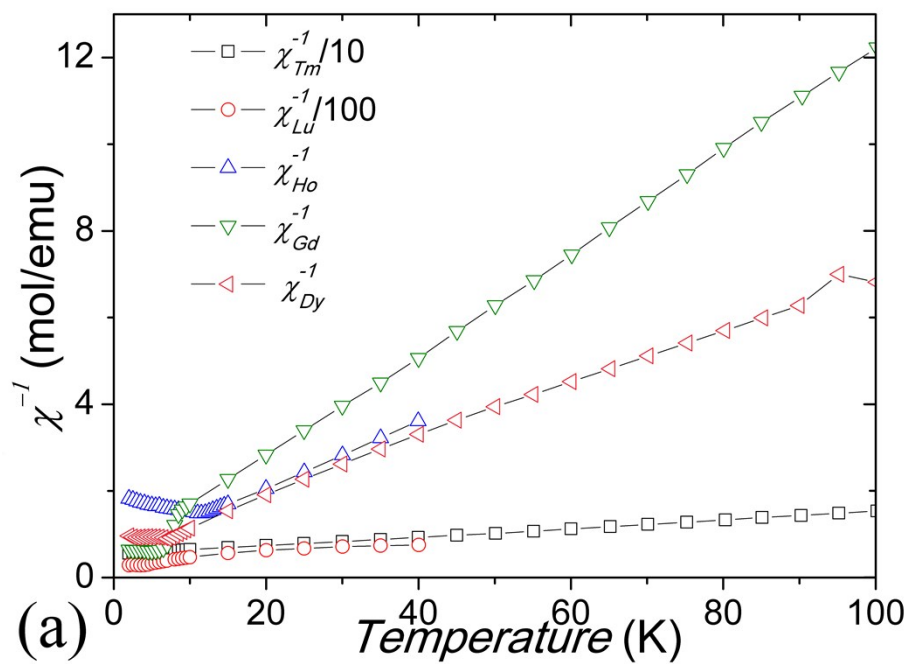


**Figure S11.** inverse susceptibility  $\chi^{-1}$  vs. temperature for  $\text{Ba}_5\text{Ln}_{1-x}\text{Mn}_{4+y}\text{O}_{15-\delta}$  (a)  $\text{Ln}=\text{Tm}, \text{Lu}, \text{Ho}, \text{Gd}$  and  $\text{Dy}$  at 20 Oe; (b)  $\text{Ln} = \text{Er}, \text{Tb}, \text{Yb}, \text{Eu}$  and  $\text{Sm}$  at 1000 Oe. For clarity,  $\chi^{-1}$  are scaled by 0.1 for the Sm, Eu and Tm samples, and by 0.01 for the Lu sample.